THE JOURNAL OF BIOLOGICAL CHEMISTRY
Vol. 275, No. 23, Issue of June 9, pp. 17510–17516, 2000

Printed in U.S.A.

A Dimer as a Building Block in Assembling RNA

A HEXAMER THAT GEARS BACTERIAL VIRUS phi29 DNA-TRANSLOCATING MACHINERY*

Received for publication, December 1, 1999, and in revised form, February 28, 2000
Published, JBC Papers in Press, March 13, 2000, DOI 10.1074/jbc.M909662199

Chaoping Chen‡§, Sitong Sheng¶, Zhifeng Shao¶, and Peixuan Guo‡‖

From the ‡Department of Pathobiology, Purdue University, West Lafayette, Indiana 47907 and the ¶Department of Molecular Physiology and Biological Physics, University of Virginia, Charlottesville, Virginia 22908

Six RNA (pRNA) molecules form a hexamer, via hand-in-hand interaction, to gear bacterial virus phi29 DNA translocation machinery. Here we report the pathway and the conditions for the hexamer formation. Stable pRNA dimers and trimers were assembled in solution, isolated from native gels, and separated by sedimentation, providing a model system for the study of RNA dimers and trimers in a protein-free environment. Cryo-atomic force microscopy revealed that monomers displayed a ⌐ outline, dimers exhibited an elongated shape, and trimers formed a triangle. Dimerization of pRNA was promoted by a variety of cations including spermidine, whereas procapsid binding and DNA packaging required specific divalent cations, including Mg^{2+}, Ca^{2+}, and Mn^{2+}. Both the tandem and fused pRNA dimers with complementary loops designed to form even-numbered rings were active in DNA packaging, whereas those without complementary loops were inactive. We conclude that dimers are the building blocks of the hexamer, and the pathway of building a hexamer is: dimer → tetramer → hexamer. The Hill coefficient of 2.5 suggests that there are three binding sites with cooperative binding on the surface of the procapsid. The two interacting loops played a key role in recruiting the incoming dimer, whereas the procapsid served as the foundation for hexamer assembly.

Multimerization of RNA molecules plays diverse roles in various biological systems. Dimerization of retrovirus RNA is believed to govern the essential steps of the retroviral life cycle, including translation, reverse transcription, RNA encapsidation, and virion assembly (1–5). During the early events of pre-mRNA splicing, there are several types of interactions through a network of RNA-RNA, RNA-protein, and protein-protein contacts (6–10). In addition, RNA-RNA interactions are involved in the cleavage of pre-tRNA by RNase P (11–13) and genetic regulation in bacteria (14, 15), eukaryotes (16), plants (17), mammals (18), and plasmids (19).

Recently, we reported that phi29 RNA interacts hand-in-hand to form hexamers to gear a DNA translocation machinery (20–27) that uses ATP as the energy source (28). Such loop-loop interaction of phi29 pRNA is different from pseudoknots (29, 30) and kissing loops (1, 3–5, 31–34) that have been characterized previously. Pseudoknots involve the intramolecular interactions within one single molecule, and kissing loops involve the interaction of two self-complementary loops to form a dimer (1–5, 36). Since phi29 pRNAs form closed rings, the intermolecular interaction of pRNAs must require that each RNA molecule contribute one loop to pair with an alternate loop of the next pRNA. The key feature of the "hand-in-hand model" is that multiple RNAs interact via alternating interlocking loops to form a closed ring. Such hand-in-hand loop-loop interactions may also play an important role in other systems as well. For example, RNA-RNA interaction via alternating loops has also been reported for *bicoid* mRNA in *Drosophila* embryos (37). We speculated that the mechanism of *bicoid* mRNA interaction and translocation might be similar to that of phi29 pRNA (26). It is possible, although not proven, that a *bicoid* mRNA may also form multimeric rings to ride, track, or rotate along Staufen protein during its transportation. Indeed, there is evidence that bicoid mRNA can form multimers (see Fig. 3 of Ref. 37).

The function of phi29 pRNA is to enable the translocation of viral genomic DNA into a preformed protein shell, *i.e.* procapsid, during replication (38–43). The secondary structure of pRNA (Fig. 1*I*) has been examined by many indirect techniques, such as phylogenetic analysis (26, 44), compensatory modification (45–50), and nuclease probing (44, 51), and partially confirmed by cross-linking (27, 51, 52). Here, we report the isolation of stable pRNA dimers and trimers and directly resolve the shapes and dimensions of pRNA monomers, dimers, and trimers by cryo-atomic force microscopy (cryo-AFM).[1] In combination with biochemical approaches, we propose a model for the assembly of pRNA hexamers.

EXPERIMENTAL PROCEDURES

Synthesis and Nomenclature of Mutant pRNAs—Methods for the synthesis of pRNA and the construction of circularly permuted pRNA (cpRNA) have been described previously (53). To facilitate the modification of the loop sequences, cpRNA 75/71, which shows a wild type phenotype (54), was used as a parental RNA. All RNAs made in this study had the same opening between C^{71} (serving as new 3′-end) and G^{75} (serving as new 5′-end), except where described otherwise. Oligo pairs carrying mutated loop sequences were used to amplify DNA fragments by PCR using the DNA template pRNA75/71. The resulting PCR product was used as the template for *in vitro* synthesis of mutant pRNAs as described (53). The mutant pRNA produced from the PCR template using primer pairs A and b, with respective loop mutations, was called pRNA A-b. Sequences of oligos used to make mutant pRNAs with interrupted right and left loops were also described previously

* This work was supported by National Science Foundation Grants MCB9723923 (to P. G.) and DBI9730060 (to Z. S.) and National Institutes of Health Grants GM59944 (to P. G.) and RRO7720 (to Z. S.) and by the Integrated Biotechnology Corp. (to P. G.). The costs of publication of this article were defrayed in part by the payment of page charges. This article must therefore be hereby marked "*advertisement*" in accordance with 18 U.S.C. Section 1734 solely to indicate this fact.

§ Current address: Dept. of Molecular Genetics and Biochemistry, University of Pittsburgh/Medical School, Pittsburgh, PA 15261.

‖ To whom correspondence should be addressed: Purdue Cancer Center, B-36 Hansen Life Science Research Bldg., Purdue University, West Lafayette, IN 47907. Tel.: 765-494-7561; Fax: 765-496-1795; E-mail: guo@vet.purdue.edu.

[1] The abbreviations used are: AFM, atomic force microscopy; cpRNA, circularly permuted pRNA; PCR, polymerase chain reaction; PAGE, polyacrylamide gel electrphoresis.

(26). The uppercase letter represents mutations in the right loop, and the lowercase letter represents mutations in the left loop. DNA templates for 5′/3′ pRNA A-b and 5′/3′ pRNA B-a, which had regular 5′/3′ ends as in the wild type pRNA, were prepared from two-step PCR (23) and cloned into the vector pGEM (Promega). Similarly, the fused and tandem (concatenated) DNA templates for the production of pRNA dimers were generated from three-step PCR and cloned into the pGEM vector as well. All mutant RNAs made by *in vitro* transcription were purified by excision from 8 M urea-denaturing gels and quantified by UV absorbance with 1 A_{260} equal to 40 μg/ml pRNA.

Native TBM Buffer (See Below)-PAGE to Detect pRNA Multimers—10% native polyacrylamide gels (51) were prepared in TBM buffer (89 mM Tris, 200 mM boric acid, 5 mM $MgCl_2$, pH 7.6). About 0.5 μg of total pRNA in TBM was loaded in each lane. Equal amounts of each of the two or three types of pRNA were used to study the formation of dimers and trimers, with the total amount of pRNA kept constant. After running at 4 °C for 3 h, the RNA was visualized by ethidium bromide staining. Images were captured using an Eagle Eye II system (Stratagene).

Isolation of Dimers and Trimers from Native PAGE—Tritiated pRNA A-b was mixed with unlabeled B-a for dimers or B-e plus E-a for trimers and subjected to electrophoresis in 10% native PAGE made in TBM. The pRNA dimer and trimer bands were excised from the gels and eluted using the same TBM buffer at 4 °C overnight. The eluted complexes were then kept in TBM buffer at 4 °C for further use or frozen at −20 °C.

Cryo-AFM of pRNA Oligomers—The oligomeric pRNA were purified from native PAGE gel. To prepare the sample for cryo-AFM imaging, a piece of mica was freshly cleaved and soaked with spermidine. Excess spermidine was removed by repeated rinse with deionized water; the pRNA sample (10 μg/ml) was applied to mica preincubated with TBM buffer. After 30 s, the unbound pRNA was removed by rinsing with the same buffer. Before the sample was transferred to cryo-AFM for imaging, it was quickly rinsed with deionized water (<1 s), and the solution was removed with dry nitrogen within several seconds (55). All cryo -AFM images were collected at 80 K, as described elsewhere (56). Scan lines were removed by an off-line matching of the basal line. Calibration of the scanner was performed with mica and 1 μm dot matrix.

Separation of pRNA Complexes by Sucrose Gradient Sedimentation—Linear 5–20% sucrose gradients were prepared in TB (TB is the TBM buffer without Mg^{2+}) buffer, pH 7.6, containing respective ions such as 5 mM $MgCl_2$ unless otherwise indicated. The pRNA mixtures containing multimers were loaded onto the top of the gradient. To separate dimers from trimers, samples were spun at 45,000 rpm for 13 h at 4 °C in a SW55 rotor. To separate dimers from monomers, samples were spun at 50,000 rpm for 14.5 h at 4 °C in a SW55 rotor. After sedimentation, fractions were collected at 15 drops each and subjected to scintillation counting.

Binding Assays for pRNAs to Procapsid—Binding assays were performed with sucrose gradient sedimentation (41). A constant amount of purified procapsids, 5 μl at 2 mg/ml, was dialyzed on a 0.025-μm VS filter (Millipore Corp.) against TBE buffer (89 mM Tris borate, 2 mM EDTA, pH 8.0) (57) for 15 min at ambient temperature. Then various amounts of [^{3}H]pRNA, dissolved in 5 μl of TMS (50 mM Tris/pH 7.8, 100 mM NaCl, 10 mM $MgCl_2$), were added. The mixture containing procapsids, and pRNA was further dialyzed against TMS buffer for another 30 min at ambient temperature. Total volume for binding assay was always kept at 10 μl to facilitate the concentration calculation and comparison of different pRNA samples. After incubation, the reaction volume was brought up to 100 μl and then loaded onto the top of a 5–20% sucrose gradient prepared in Tris-saline buffer with specified ions of interest, such as 10 mM $MgCl_2$, in most cases. After 35 min of centrifugation in an SW55 rotor at 35,000 rpm at 9 °C, fractions were collected from the bottom of the tube and subjected to liquid scintillation counting.

Competition Assay for Dimer Binding—Purified procapsids 5 μl (2 mg/ml) in TMS were dialyzed against TBE on a 0.025-μm VS filter at ambient temperature for 15 min. 1.25 μg of [^{3}H]A-b/B-a RNAs were mixed with variable amounts of unlabeled competitors in 3 μl of TMS and dried by vacuum. Then the RNAs were mixed with 5 μl of procapsids that had been dialyzed against TBE for 15 min. The maximum binding volume was limited to 5 μl to maintain the molar concentration

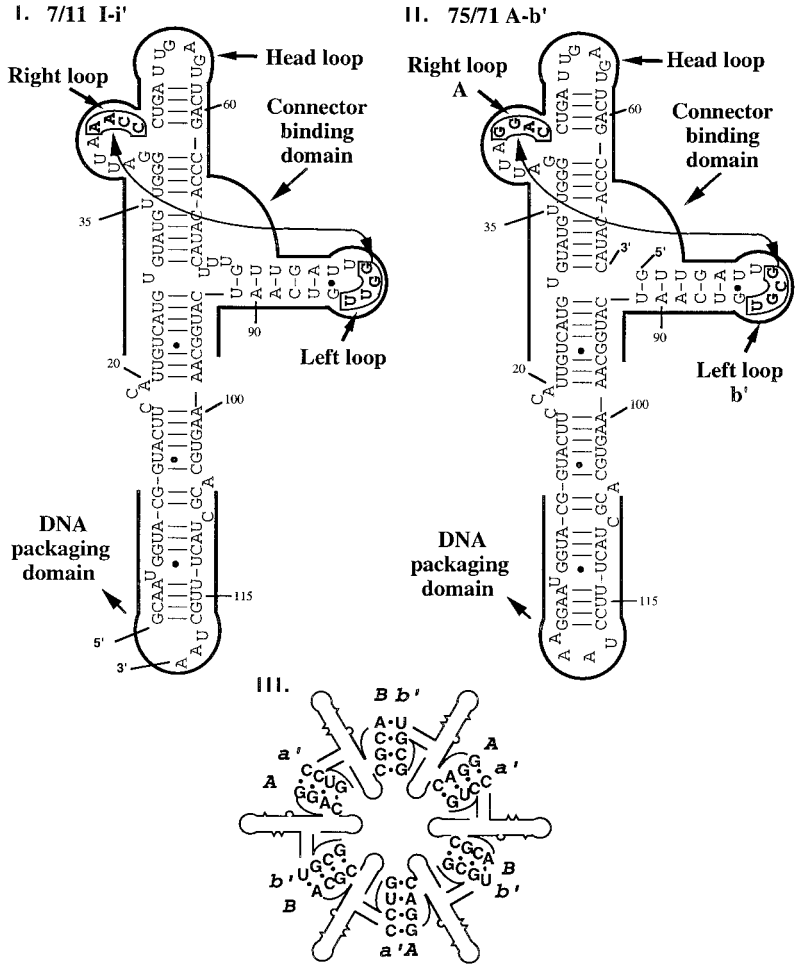

FIG. 1. Primary sequences and predicted secondary structure of wild-type phenotype pRNA 7/11 (*I*) and circularly permuted cpRNA 75/71 (*II*). Bases $U^{72}U^{73}U^{74}$ are deleted, and G^{75} and C^{71} serve as new 5′ and 3′ ends, respectively. Right hand and left hand loops involved in hand-in-hand interaction are *boxed* and in *bold*. Two functional domains are *outlined*, and the numbering is the same as in wild type pRNA. *III*, formation of hexameric pRNA by interaction of the right and left hand loops from pRNA pairs A-b and B-a.

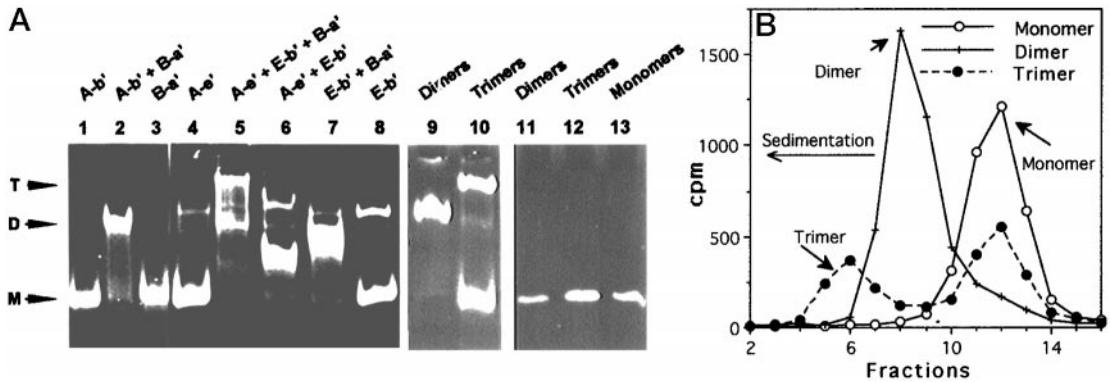

FIG. 2. *A*, native polyacrylamide gel showing dimeric and trimeric complexes in TBM buffer containing 5 mM Mg^{2+} (*lanes 1–10*). Monomers (*M*), dimers (*D*), and trimers (*T*) are indicated by *arrows*. The pRNAs were mixed in equal molar concentrations when more than one pRNA was used. Dimeric and trimeric pRNA isolated from 10% TBM native gel were re-run in 10% native gel (*lanes 9–10*) and 10% denaturing gel (*lanes 11–13*). *B*, 5–20% sucrose gradient sedimentation of [^{3}H]pRNA dimers and trimers purified from native gels.

of pRNAs for up to several μM. After dialysis for another 30 min against TMS at ambient temperature, 95 μl of TMS was added to bring the volume to 100 μl, and the mixtures were then subjected to sedimentation via 5–20% sucrose gradient made in TMS to separate procapsid-bound pRNAs from unbound ones.

In Vitro phi29 Virion Assembly Assay—The purification of procapsids (58, 59), gp16 (60), DNA-gp3 (57), the preparation of neck and tail proteins (61), and the assembly of infectious phi29 virion *in vitro* (57) have been described previously. Briefly, 1.5 μl of purified procapsids (2 mg/ml) was dialyzed on a 0.025-μm VS filter against TBE for 15 min at ambient temperature. Various amounts of pRNAs, including monomers and dimers, dissolved in 1.5 μl of TMS buffer, were added to procapsids. The mixtures were then dialyzed against TMS for another 30 min. A small volume was used to ensure high concentration of pRNAs in the reaction. The pRNA-enriched procapsids were mixed with gp16, DNA-gp3, and reaction buffer (10 mM ATP, 6 mM 2-mercaptoethanol, 3 mM spermidine in TMS) to complete the DNA packaging reaction. After 30 min, neck, tail, and morphogenic proteins were added to the DNA packaging reactions to complete assembly of infectious virions, which were assayed by standard plaque formation.

RESULTS

To simplify the description, we use uppercase letters to represent the right loop of the pRNA and lowercase to represent the left loop (Fig. 1). The same letters in upper- and lowercase indicate complementary sequences, whereas different letters indicate non-complementary loops. For example, pRNA A-a represents a pRNA with complementary right loop A (5′-GGAC^{48}) and left loop a (3′-CCUG^{82}), whereas pRNA A-b represents a pRNA with unpaired right loop A and left loop b (3′-UGCG^{82}).

Formation of pRNA Dimers and Trimers Detected by Native Gels—All pRNAs with non-complementary left and right loop sequences such as A-b, B-a, A-e, E-a, or B-e, appeared predominantly as "fast" migrating bands in native gels and, thus, were predicted to be monomers (Fig. 2*A*). However, when A-b was mixed with equal molar ratios of B-a, most of the RNAs shifted into a slower migrating band estimated to be composed of dimers. Mixing other pairs of pRNAs, *e.g.* B-e with E-b and L-j with J-l, that were predicted to form a closed ring by hand-in-hand interaction of two pairs of interlocking loops showed similar dimer bands (data not shown). In addition, when three pRNAs with interlocking loops such as A-e/E-b/B-a, which were predicted to form a closed circle by hand-in-hand interaction, were mixed with a ratio of 1:1:1, a band with a migration rate slower than that of the dimer was observed (Fig. 2*A*, *lane 5*). This band represented trimers.

The pRNA A-e and E-b contain only one pair, not two, of complementary interacting loops (E and e). These two pRNAs, with other two unpaired A and b loops, could not form a closed circle due to the mismatch of A and b. It is thus called an "open dimer." When mixed at equal molar concentration, *A-e* + *E-b* showed a smear between dimer and monomer bands (Fig. 2*A*, *lane 6*). A similar phenomenon was also observed with other open dimers, such as *E-b* + *B-a* (Fig. 2*A*, *lane 7*) and *B-e* + *E-a* (data not shown). These data suggested that the formation of a closed ring by hand-in-hand interaction was required for the formation of stable dimeric complexes in solution. Open dimers were unstable in native gels, and the smear may result from the dissociation of horseshoe-shaped dimers during electrophoresis. The minor dimeric band from the sample *E-b* alone (*lane 8*) was generated by nonspecific sequence interactions (see "Discussion" of Ref. 26).

Closed Dimers and Trimers Are Stable in Solution after Purification from Native Gels—Closed dimers [^{3}H]pRNA A-b/B-a and trimers [^{3}H]pRNA A-b/B-e/E-a were isolated from native gels (see "Experimental Procedures") and were electrophoresed again in a native gel containing Mg^{2+} (Fig. 2*A*, *lanes 9* and *10*) as well as in a denaturing gel containing EDTA (Fig. 2*A*, *lanes 11–13*). The dimeric A-b/B-a species remained predominately as dimers in the native gel, whereas the majority of the trimers remained intact with about 15% of them dissociated into monomers. These results indicate that pRNA dimers are more stable than trimers. When run under denaturing conditions, both dimers and trimers showed only a monomer band (Fig. 2*A*, *lanes 11* and *12*). When Mg^{2+} was absent, no dimer or trimer band was detected (data now shown), suggesting that dimerization and trimerization required Mg^{2+}.

Additionally, each sample was then subjected to sedimentation through a 5–20% sucrose gradient in TBM buffer. [^{3}H]pRNA A-b alone served as a monomer control. The monomers centered at fraction 12, whereas the dimers and trimers at centered at fractions 8 and 6, respectively (Fig. 2*B*). A plot of hypothetical molecular weight *versus* the log of migration distance (fraction number) in the gradient showed a linear relationship. Thus the peak at fractions 12, 8, and 6 represented monomers, dimers, and trimers, respectively. This result supports our prediction that mixing pRNA A-b with B-a produced dimers and mixing A-b with B-e and E-a produced trimers.

The isolated closed dimers were centered at fraction 8 without any additional peaks, indicating that no dissociation occurred during sedimentation. However, most of the open dimers, including B-a/A-e, E-b/B-a, I-a/A-b, and A-b/B-e only showed monomeric peaks at fraction 12 (data not shown). The data suggest that closed dimers are more stable than open dimers, which are unable to form a dimer peak in sucrose gradients, although they could form some smears in native gels (Fig. 2*A*). The isolated trimers showed two peaks at fraction 12 and 6, respectively, after sucrose gradient sedimentation.

About 60% of the label was centered at fraction 12, corresponding to monomers. This suggests that the isolated trimers are not as stable as the closed dimers under the conditions tested or the formation of trimers is a concentration-dependent process (see "Discussion"). Although trimers dissociated into monomers, there was no open dimer intermediate observed in the sucrose gradient. This is consistent with the finding that open dimers were unstable, because the dimers resulting from the dissociation of such trimer are open dimers.

Cryo AFM also directly confirmed the existence of dimers and trimers (Fig. 3). The pRNA monomers folded into a ✔-shaped structure, A-b/B-a dimers had an elongated shape, and trimers showed a triangular appearance. The monomers were 16.7 ± 0.9 nm long, and the dimers were 30.2 ± 2.5 nm long and 11.6 ± 1.4 nm wide. Trimers were 30.3 ± 2.4 nm on each side. Because AFM measurements tend to be an overestimate, the actual size of the molecules should be slightly smaller. It should be pointed out that the formation of dimers and trimers requires the presence of Mg^{2+} in solution. However, for cryo-AFM, precipitation of salts on the surface would interfere with imaging. Therefore, samples were briefly rinsed with water (<1 s) before being frozen. This step had resulted in some dissociation of dimers and trimers even when pRNAs were already adsorbed to the mica surface.

Effect of Mono and Divalent Cations on pRNA Dimer Formation, Procapsid Binding, and Viral Assembly—The dependence of dimer formation on Mg^{2+} was investigated further (Fig. 4*A*). For cpRNAs with G^{75} as the 5′-end and C^{71} as the 3′-end, the

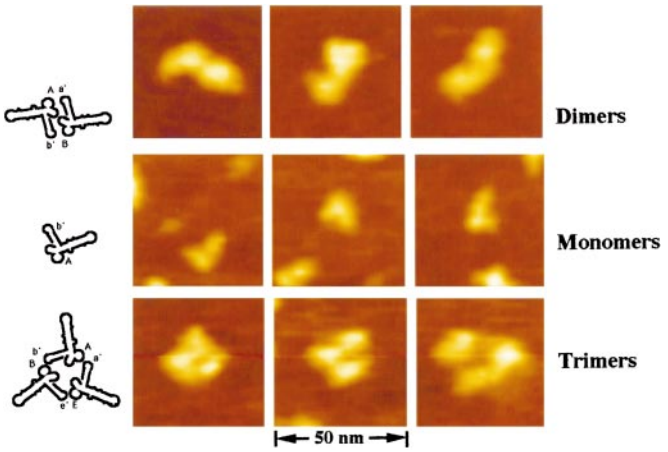

FIG. 3. **Cryo AFM images of pRNA dimers, monomers, and trimers.** The image was color-coded for topograph. The *bright regions* correspond to the thick part of the molecule. The images clearly indicate that the area around the head loop, the elbow of the ✔, is the thickest.

TABLE I
Effects of cations on pRNA dimer formation, procapsid binding, and virion assembly

	Dimer formation		Binding activity		Assembly 10 mM
	5 mM	1 M	10 mM	1 M	
	%		%		*ptu/ml*
Monovalent					
LiCl	<5	79		0	0
NaCl	<5	60		0	0
KCl	<5	48		0	0
Divalent					
$MnCl_2$	73		2		1.6×10^4
$CaCl_2$	68		10		3.4×10^6
$MgCl_2$	50		9		3.3×10^7
$SrCl_2$	37		⇓[a]		0
$CoCl_2$	<5		<1		0
$NiCl_2$	<5		<1		0
$ZnCl_2$	⇓		⇓[a]		0
Spermidine	60		0		0

[a] Precipitation.

TABLE II
Packaging activities of pRNA dimers

Designed pRNAs	Packaging activity (pfu/ml)
Wild type pRNA	2.0×10^7
Fused dimer	2.2×10^5
Tandem dimer	Ii'/Ii': 5.1×10^5 Ab'/Ab': 0 Ab'/Ba': 2.0×10^5
No pRNA	0

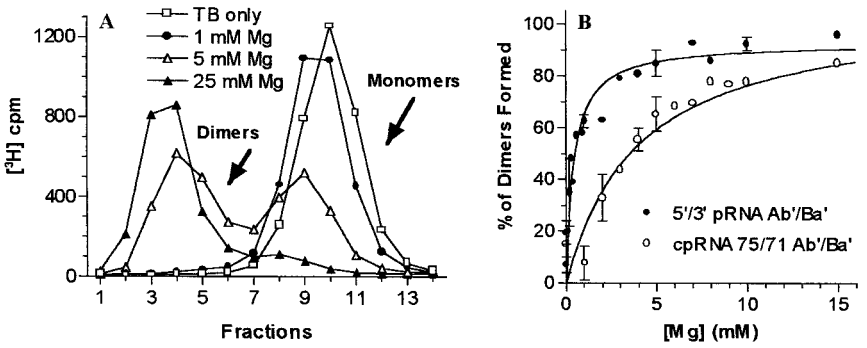

FIG. 4. **Effect of Mg^{2+} concentration on pRNA dimerization and procapsid binding.** *A*, sucrose gradient sedimentation of [^{3}H]pRNA A-b and B-a mixture with variable concentrations of Mg^{2+}. *TB*, TBM buffer without Mg^{2+}. *B*, Mg^{2+} dependence of dimerization of cpRNA 75/71 A-b with B-a (*open circle*) and pRNA A-b with B-a containing regular 5′/3′ end (*solid circle*), evaluated by sucrose gradient sedimentation. The Mg^{2+} concentration for 50% pRNAs dimer formation was 4 mM and 0.4 mM for cpRNA and 5′/3′ pRNA, respectively, as determined by nonlinear regression analysis of GraphPad Prism 2.01.

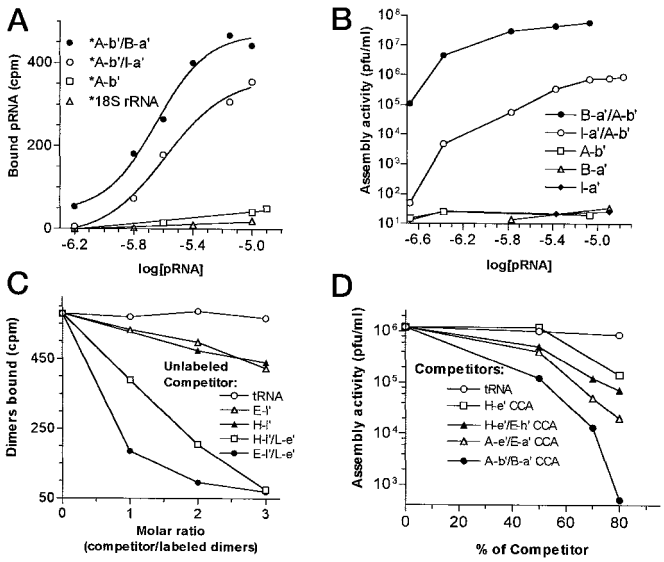

FIG. 5. Procapsid binding (*A*) and virion assembly (*B*) activities of monomer, open dimer, and closed dimers tested by sucrose gradient sedimentation and *in vitro* assembly assay. The concentrations of pRNA used represents the monomers in reaction. *C*, competition of procapsid binding of pRNA A-b/B-a by a variety of RNAs. Increasing amounts of unlabeled competitor RNAs were mixed with constant amounts of [^{3}H]pRNA A-b/B-a. The closed dimer (pRNA E-l/L-e) and tRNA served as positive and negative controls, respectively. *D*, competition and inhibition of inactive dimers (CCA dimers) with active dimers (pRNA A-b/B-a) in viral assembly. A constant amount (0.3 μg) of total pRNAs was used in each reaction in phi29 assembly mixture containing variable percentages of competitor pRNA, with tRNA as the negative control.

Mg^{2+} concentration required for 50% dimer formation was 4 mM, whereas for pRNAs with wild type 5′/3′ ends, it was 0.4 mM (Fig. 4*B*). The data suggested that the Mg^{2+} requirements for dimer formation is different between circularly permuted pRNAs and pRNAs with regular ends. It is possible that more Mg^{2+} ions were required for cpRNAs to fold into appropriate conformations due to a new opening in the middle of pRNAs, whereas pRNAs with regular ends would fold into the corresponding conformation more favorably. Therefore, the Mg^{2+} requirement for dimer formation of regular pRNAs is 10-fold less than that of circularly permuted pRNAs.

Effects of other cations on dimer formation, procapsid binding, and viral assembly were also studied using the pRNA pair A-b and B-a (Table I). At least a 1 M concentration in monovalent ions was required for dimerization, whereas as low as a 5 mM concentration of divalent ions was sufficient. Spermidine, a positively charged compound could also stimulate dimer formation at a concentration of 5 mM, indicating that dimerization is a result of a cation effect. Dimerization was not detected when $CoCl_2$ or $NiCl_2$ were used. $FeCl_2$, $ZnCl_2$, or $CdCl_2$ caused the precipitation of pRNA. These data suggest that pRNAs tend to form dimers in the presence of positively charged cations, including mono- or divalent cations as well as spermidine. It seems that dimer formation is an intrinsic feature of pRNAs, and cations only play a facilitating role.

In contrast to dimer formation, binding of dimers to procapsid showed a more specific requirement for divalent cations. Neither monovalent cations nor spermidine could promote the binding of dimers to procapsids. Only Mg^{2+} and Ca^{2+} could promote such binding, whereas Mn^{2+} showed a reduced binding efficiency. These data indicate that dimer formation is not sufficient for procapsid binding, DNA packaging, and viral assembly (Table I). Specific divalent cations, Mg^{2+}, Ca^{2+}, and Mn^{2+}, play further roles in addition to facilitating dimer formation.

Covalently Linked Dimeric pRNAs Were Able to Package DNA in Vitro—To further verify that dimers are the building blocks of RNA hexamer, we constructed several dimeric pRNAs. First, a fused pRNA dimer was generated such that two pRNAs were covalently linked together by merging the right and left loop sequences directly (Table II). Interestingly, the fused pRNA dimers were active in phi29 assembly. In addition, tandem pRNAs, in which two pRNAs are covalently linked head to tail, showed similar activities. It is worth mentioning that a tandem pRNA A-b-A-b was inactive, even though two pRNAs were covalently held together. This is consistent with the previous observation that base pairing between the right and left loops is critical for dimer and hexamer formation (23). Both tandem pRNA I-i-I-i and A-b-B-a had complementary loop sequences, and they were able to form dimers and remained active in DNA packaging (Table II). Results from both fused and tandem pRNAs suggest that dimers are the building units in hexamer formation.

pRNA Monomers with Unpaired Right and Left Loops Were Incompetent in Dimer Formation, Procapsid Binding, and Viral Assembly—To test the binding affinity of monomers with unpaired right and left loops, increasing amounts of pRNA [^{3}H]A-b monomers were incubated with constant amounts of procapsid. Procapsid-bound RNAs were separated from unbound RNA by sedimentation and were counted. The A-b monomers showed the same binding affinity as the nonspecific control, 18 S rRNA (Fig. 5*A*). Similarly, the A-b monomers were inactive in DNA packaging tested by *in vitro* assembly (Fig. 5*B*). The data indicated that pRNA monomers with non-complementary right and left loops could not bind to procapsids because they were incompetent to form dimers in solution. Consequently, very few or no infectious virion were assembled, since the monomers were not able to bind procapsid. Again, the data support our conclusion that dimers are the basic unit for procapsid binding.

Open Dimers Can Bind to Procapsids and Package DNAs at Reduced Activities—Unlike monomers with interrupted right and left loops, both closed dimers and open dimers were able to bind to procapsids. The closed dimers A-b/B-a had the highest binding affinity and reached a plateau at a pRNA concentration of about 2.5 μM. Open dimers A-b/I-a could bind to procapsids, but with a moderate strength (Fig. 5, *A* and *B*). After reaching the plateau, binding of the open dimers accounted for 75% that of closed dimers. Mismatches between open dimers might decrease the cooperativity of binding, as demonstrated by the reduced Hill coefficient of open dimers (Fig. 6). These data imply that dimers are the binding unit, and a complementary loop is needed for the recruitment of a subsequent dimer in forming the hexamer.

Communication between the right and left loops is also required for DNA packaging. We used extremely high concentrations of pRNA to saturate all procapsids in *in vitro* assembly (Fig. 5*B*). Open dimers showed about a 100-fold reduction in assembly activity compared with closed dimers. Considering that there is only about a 25% reduction in procapsid binding (Fig. 5*A*), interaction between right and left loops must play other roles during the DNA packaging process, and disruption of such interaction causes further reduction in the assembly activity.

Competitive Binding Assay of Open and Closed Dimers—Competition binding assays were performed to determine whether the dimer is the minimal binding unit. Constant amounts of dimeric [^{3}H]pRNA A-b/B-a were mixed with increasing amounts of three kinds of unlabeled competitors: monomers, open dimers, or closed dimers (Fig. 5*C*). Monomers, including E-l, L-e, and H-l, which cannot form open dimers

with either A-b or B-a, were extremely weak in competing with dimers for procapsid binding, suggesting that monomers cannot bind to the procapsid. The second class of competitor was closed dimers such as E-l/L-e, which could form a cyclic form by themselves but do not contain complementary loops to interlock with [^{3}H]A-b/B-a. When increasing amounts of E-l/L-e were mixed with [^{3}H]A-b/B-a dimers, binding of [^{3}H]A-b/B-a dimers to procapsids decreased dramatically. This result indicates that closed dimers are strong competitors for procapsid binding. The third class of competitors was open dimers of the type H-l/L-e. Although the inhibition efficiency of open dimers for procapsid binding was not as strong as that of closed dimers, they were nevertheless able to compete with [^{3}H]A-b/B-a dimers for procapsid binding (Fig. 5*C*, *open square*). Again, these data indicate that the dimer is the basic procapsid binding unit and that interactions between the right and left loops through base pairing plays further roles in recruiting incoming dimers.

The addition of unlabeled A-b/B-a or A-b/B-c to the reaction containing [^{3}H]pRNA A-b/B-a could change the final concentration of A-b. Due to the fact that binding to the procapsid is a concentration-dependent reaction, the use of unlabeled A-b/B-a or A-b/B-c to compete with [^{3}H]A-b/B-a dimers is not plausible and will not be addressed in this report.

Competition Inhibition of Viral Assembly Also Suggests Sequential Addition of Dimers in Hexamer Formation—If dimers are the building blocks, there are two possible pathways to assemble a hexamer. The first one is the independent addition of individual dimers ($2 \times 3 = 6$). The second one is sequential addition of dimers through hand-in-hand interaction to recruit the incoming dimers ($2 + 2 + 2 = 6$). To determine the pathway of hexamer assembly, competition and inhibition assays were carried out by using CCA dimers (23). CCA dimers are fully active in procapsid binding but inactive in DNA packaging and should be able to compete with the active dimeric pRNA A-b/B-a for procapsid binding (Fig. 5*D*). The A-b/B-a CCA dimers did compete with A-b/B-a dimers for procapsid binding in hexamer formation by incorporating into the complex and strongly inhibited virion assembly (Fig. 5*D*, *solid line*). The pRNA A-e/E-a CCA dimer, which contains only one complementary loop to interact with the A-b/B-a dimer, showed a reduced inhibition efficiency. The H-e/E-h CCA dimer, which does not contain complementary hand-in-hand loops to pair with A-b/B-a dimer, displayed the lowest inhibition efficiency. The monomer pRNA H-e CCA showed a very low inhibition efficiency. These results support the second pathway, since if dimers had incorporated into hexamers independently without hand-in-hand interaction, all three CCA dimers should have shown equal inhibition efficiency. These data suggest that hand-in-hand interaction plays a role in recruiting the in-coming dimers.

Hill Plot Analysis of pRNA Binding Curves Supports Cooperative Binding of Dimers—Hill plot analysis was further performed to evaluate the cooperativity in hexamer formation using dimers (Fig. 6). Although the K_m of each type of RNA varies, the Hill coefficients of pRNA 7/11 monomers, which has the wild type phenotype, as well as purified dimers and trimers were 2.52 ± 0.83, 2.56 ± 0.38, 2.55 ± 0.62, respectively. That is, the Hill coefficients of all of these three fully active RNAs were close to 2.5. Generally, a Hill coefficient between 2 and 3 implies two possibilities. The first is that, for each procapsid, there were three binding sites for dimers and the binding is cooperative (62). The second is that the number of binding sites is more than three, whereas the cooperativity in binding is limited. Because six pRNAs bind to each procapsid (20, 21, 23), it is reasonable to consider and accept the first possibility. This positive cooperativity can explain the lower binding efficiency of open dimers, which was 2.16 ± 0.42, since the mismatches between the corresponding right and left loops could hinder the cooperativity in recruiting subsequent dimers.

The apparent K_m values of pRNA 7/11 trimers, dimers, and open dimers were analyzed by GraphPad Prism 2.01 as 0.08 ± 0.01 μM, 0.69 ± 0.1 μM, 2.73 ± 1.1 μM, and 2.63 ± 1.2 μM, respectively. Different K_m values only denote the difference in the concentration requirement for these RNAs to form dimers suitable for procapsid binding and hexamer assembly. They did not change the pathway or the pattern of cooperative addition

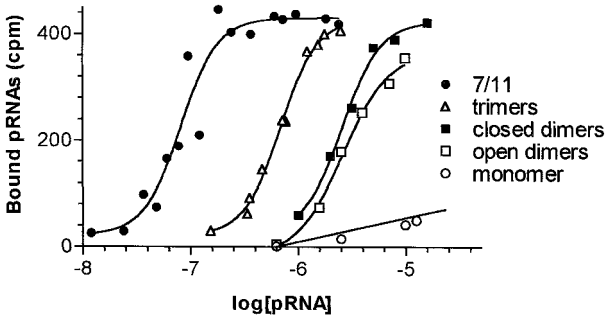

FIG. 6. **Procapsid binding constants of pRNAs by Hill analysis using Prism 2.01.** A constant amount of procapsid was mixed with increasing amounts of different RNAs, including wild type phenotype pRNA 7/11 (*solid circle*), isolated trimers (*triangle*), closed dimers (*solid square*), open dimers (*open square*), and monomers (*open circle*). All of the pRNAs including 7/11, trimers, and closed dimers showed a similar Hill coefficient, namely 2.52 ± 0.83, 2.56 ± 0.38, 2.55 ± 0.62, respectively, whereas the open dimers showed a lower Hill coefficient, 2.16 ± 0.42. The apparent K_m values were determined by GraphPad Prism 2.01 as 0.08 ± 0.01 μM (pRNA 7/11), 0.69 ± 0.1 μM (trimers), 2.63 ± 1.2 μM (open dimers), and 2.73 ± 1.1 μM (closed dimers), respectively. Each curve was the result of at least two independent experiments. The fitness value of R^2 was close to 0.99.

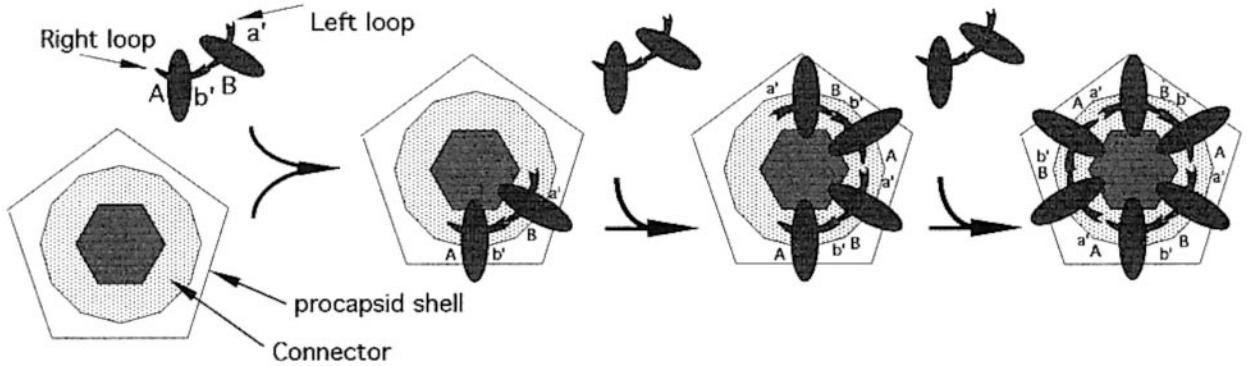

FIG. 7. **A diagram depicts the pathway of pRNA hexamer formation.** The *pentagon* represents the procapsid shell with a 5-fold symmetry. The dodecagon represents the connector with a 6-fold central hole (35, 64, 65). The *black ellipses* represent the pRNA.

of each dimer. Therefore, the Hill coefficients of each species are similar.

DISCUSSION

This study was focused on the condition and the pathway for the assembly of the pRNA hexamer. It was found that pRNAs containing complementary loops, either within one pRNA (such as monomer I-i) or between two pRNAs (such as A-b/B-a) could bind to procapsid and package DNA efficiently. Those pRNAs that did not contain the complementary loops, such as A-b by itself or the pair H-i/L-e, were incompetent in procapsid binding and DNA packaging. Dimers purified from gels were able to bind to procapsid and to package DNA. The Hill coefficient of 2.5 suggests that on the surface of the procapsid there are three binding sites with cooperative binding. Competition assays revealed that procapsid binding and DNA packaging were efficiently inhibited by dimer competitors with complementary loops but not by monomers or dimers with non-complementary loops. The fact that the minimum size of pRNA for procapsid binding is the same as the minimum size for dimer formation (26, 63) also supports the conclusion that dimers are the binding unit for hexamer assembly. Furthermore, covalently linked pRNA dimers were able to bind procapsid and to package DNA (27). All of these results support the following conclusions. 1) Dimers are the building blocks in hexamer formation, 2) the pathway in building a hexamer is dimer → tetramer → hexamer, and 3) the two interacting loops play key roles in recruiting the incoming dimer (Fig. 7).

If dimers are the building blocks, how can the findings that trimers could be formed from A-e, E-b, and B-a and the fact that purified trimers were able to bind procapsid and package DNA be explained? The AFM images in Fig. 3 revealed that A-e/E-b/B-a is present in solution as a triangle. Since A-e/E-b/B-a can be viewed as three open dimers, A-e/E-b, B-a/A-e, or E-b/B-a, the interface could have a three-dimensional structure similar to the dimer for procapsid binding. It was also found that tetramers, pentamers, and hexamers were present in the solution (23). Recent investigation has revealed that the formation of trimer, tetramer, pentamer, and hexamer ladders requires special conditions.[2] Clearly, this is a very unique and special RNA that will lead to discoveries of many interesting phenomena and properties concerning RNA structure and function.

Acknowledgments—We thank Dr. Elke Scholz and Lisa Huang for procapsid purification, Dr. James N. Weiss for interpretation of Hill plot analysis, and Dr. Chengguo Wang for cloning and sequencing fused and tandem pRNAs.

REFERENCES

1. Sundquist, W. I., and Heaphy, S. (1993) *Proc. Natl. Acad. Sci. U. S. A.* **90,** 3393–3397
2. Skripkin, E., Paillart, J. C., Marquet, R., Ehresmann, B., and Ehresmann, C. (1994) *Proc. Natl. Acad. Sci. U. S. A.* **91,** 4945–4949
3. Homann, M., Rittner, K., and Sczakiel, G. (1993) *J. Mol. Biol.* **233,** 7–15
4. Chang, K. Y., and Tinoco, I., Jr. (1994) *Proc. Natl. Acad. Sci. U. S. A.* **91,** 8705–8709
5. Jossinet, F., Paillart, J. C., Westhof, E., Hermann, T., Skripkin, E., Lodmell, J. S., Ehresmann, C., Ehresmann, B., and Marquet, R. (1999) *RNA* (*N. Y.*) **5,** 1222–1224
6. Berglund, J. A., Abovich, N., and Rosbash, M. (1998) *Genes Dev.* **12,** 858–867
7. Verma, M., Kurl, R. N., Blass, C., and Davidson, E. A. (1997) *Cancer Biochem. Biophys.* **15,** 211–220
8. Valcarcel, J., Gaur, R. K., Singh, R., and Green, M. R. (1996) *Science* **273,** 1706–1709
9. Frilander, M. J., and Steitz, J. A. (1999) *Genes Dev.* **13,** 851–863
10. Sontheimer, E. J., and Steitz, J. A. (1993) *Science* **262,** 1989–1996
11. Guerrier-Takada, C., Gardiner, K., Marsh, T., Pace, N., and Altman, S. (1983) *Cell* **35,** 849–857
12. Oh, B. K., and Pace, N. R. (1994) *Nucleic Acids Res.* **22,** 4087–4094
13. Baer, M. F., Reilly, R. M., McCorkle, G. M., Hai, T. Y., Altman, S., and RajBhandary, U. L. (1988) *J. Biol. Chem.* **263,** 2344–2351
14. Henkin, T. M. (1996) *Annu. Rev. Genet.* **30,** 35–57
15. Lease, R. A., Cusick, M. E., and Belfort, M. (1999) *Proc. Natl. Acad. Sci. U. S. A.* **95,** 12456–12461
16. Moss, E. G., Lee, R. C., and Ambros, V. (1997) *Cell* **88,** 637–646
17. Jorgensen, R. A., Atkinson, R. G., Forster, R. L., and Lucas, W. J. (1998) *Science* **279,** 1486–1487
18. Panning, B., and Jaenisch, R. (1998) *Cell* **93,** 305–308
19. Eguchi, Y., and Tomizawa, J. (1990) *Cell* **60,** 199–209
20. Chen, C., and Guo, P. (1997) *J. Virol.***71,** 3864–3871
21. Trottier, M., and Guo, P. (1997) *J. Virol.***71,** 487–494
22. Chen, C., Trottier, M. C., and Guo, P. (1997) *Nucleic Acids Symp. Ser.* **36,** 190–193
23. Guo, P., Zhang, C., Chen, C., Trottier, M., and Garver, K. (1998) *Mol. Cell.* **2,** 149–155
24. Zhang, F., Lemieux, S., Wu, X., St.-Arnaud, S., McMurray, C. T., Major, F., and Anderson, D. (1998) *Mol. Cell.* **2,** 141–147
25. Hendrix, R. W. (1998) *Cell* **94,** 147–150
26. Chen, C., Zhang, C., and Guo, P. (1999) *RNA* (*N. Y.*) **5,** 805–818
27. Garver, K., and Guo, P. (2000) *J. Biol. Chem.* **275,** 2817–2824
28. Guo, P., Peterson, C., and Anderson, D. (1987) *J. Mol. Biol.* **197,** 229–236
29. Pleij, C. W. A., and Bosch, L. (1989) *Methods Enzymol.* **180,** 289–303
30. Studnicka, G. M., Rahn, G. M., Cummings, I. W., and Salser, W. A. (1978) *Nucleic Acids Res.* **5,** 3365–3387
31. Prats, A. C., Roy, C., Wang, P. A., Erard, M., Housset, V., Gabus, C., Paoletti, C., and Darlix, J. L. (1990) *J. Virol.* **64,** 774–783
32. Bender, W., and Davidson, N. (1976) *Cell* **7,** 595–607
33. Chang, K. Y., and Tinoco, I., Jr. (1997) *J. Mol. Biol.* **269,** 52–66
34. Laughrea, M., Jette, L., Mak, J., Kleiman, L., Liang, C., and Wainberg, M. A. (1997) *J. Virol.* **71,** 3397–3406
35. Jimenez, J., Santisteban, A., Carazo, J. M., and Carrascosa, J. L. (1986) *Science* **232,** 1113–1115
36. Clever, J. L., Wong, M. L., and Parslow, T. G. (1996) *J. Virol.* **70,** 5902–5908
37. Ferrandon, D., Koch, I., Westhof, E., and Nusslein-Volhard, C. (1997) *EMBO J.* **16,** 1751–1758
38. Guo, P., Erickson, S., and Anderson, D. (1987) *Science* **236,** 690–694
39. Herranz, L., Salas, M., and Carrascosa, J. L. (1986) *Virology* **155,** 289–292
40. Donate, L. E., Valpuesta, J. M., Rocher, A., Mendez, E., Rojo, F., Salas, M., and Carrascosa, J. L. (1992) *J. Biol. Chem.* **267,** 10919–10924
41. Guo, P., Bailey, S., Bodley, J. W., and Anderson, D. (1987) *Nucleic Acids Res.* **15,** 7081–7090
42. Guo, P., and Trottier, M. (1994) *Semin. Virol.* **5,** 27–37
43. Guo, P. (1994) *Semin. Virol.* **5,** 1–3
44. Bailey, S., Wichitwechkarn, J., Johnson, D., Reilly, B., Anderson, D., and Bodley, J. W. (1990) *J. Biol. Chem.* **265,** 22365–22370
45. Zhang, C. L., Lee, C.-S., and Guo, P. (1994) *Virology* **201,** 77–85
46. Zhang, C. L., Tellinghuisen, T., and Guo, P. (1995) *RNA* (*N. Y.*) **1,** 1041–1050
47. Trottier, M., Zhang, C. L., and Guo, P. (1996) *J. Virol.* **70,** 55–61
48. Wichitwechkarn, J., Bailey, S., Bodley, J. W., and Anderson, D. (1989) *Nucleic Acids Res.* **17,** 3459–3468
49. Reid, R. J. D., Bodley, J. W., and Anderson, D. (1994) *J. Biol. Chem.* **269,** 5157–5162
50. Reid, R. J. D., Zhang, F., Benson, S., and Anderson, D. (1994) *J. Biol. Chem.* **269,** 18656–18661
51. Chen, C., and Guo, P. (1997) *J. Virol.***71,** 495–500
52. Mohammad, T., Chen, C., Guo, P., and Morrison, H. (1999) *Bioorg. Med. Chem. Lett.* **9,** 1703–1708
53. Zhang, C. L., Trottier, M., and Guo, P. X. (1995) *Virology* **207,** 442–451
54. Zhang, C. L., Tellinghuisen, T., and Guo, P. (1997) *RNA* (*N. Y.*) **3,** 315–322
55. Han, W., Mou, J., Sheng, J., Yang, J., and Shao, Z. (1995) *Biochemistry* **34,** 8215–8220
56. Zhang, Y., Sheng, S., and Shao, Z. (1996) *Biophys. J* **71,** 2168–2176
57. Lee, C. S., and Guo, P. (1994) *Virology* **202,** 1039–1042
58. Guo, P., Rajogopal, B., Anderson, D., Erickson, S., and Lee, C.-S. (1991) *Virology* **185,** 395–400
59. Guo, P., Erickson, S., Xu, W., Olson, N., Baker, T. S., and Anderson, D. (1991) *Virology* **183,** 366–373
60. Guo, P., Grimes, S., and Anderson, D. (1986) *Proc. Natl. Acad. Sci. U. S. A.* **83,** 3505–3509
61. Lee, C. S., and Guo, P. (1995) *J. Virol.* **69,** 5018–5023
62. Weiss, J. N. (1997) *FASEB J.* **11,** 835–841
63. Garver, K., and Guo, P. (1997) *RNA* (*N. Y.*) **3,** 1068–1079
64. Valpuesta, J. M., Fernandez, J. J., Carazo, J. M., and Carrascosa, J. L. (1999) *Structure Fold Des.* **7,** 289–296
65. Guasch, A., Pous, J., Parraga, A., Valpuesta, J. M., Carrascosa, J. L., and Coll, M. (1998) *J. Mol. Biol.* **281,** 219–225

[2] C. Chen and P. Guo, unpublished data.